MEMBRANE CURRENT NOISE IN LOBSTER AXON UNDER VOLTAGE CLAMP

DENIS J. M. POUSSART

From the Research Laboratory of Electronics, Massachusetts Institute of Technology, Cambridge, Massachusetts 02139. Dr. Poussart's present address is the Département de Génie Électrique et Centre de Recherches en Bionique, Université Laval, Québec, Canada.

ABSTRACT Random fluctuations in the steady-state current of neural membrane were measured in the giant lobster axon by means of a low noise voltage-clamp system. The power density spectrum $S(f)$ of the fluctuations was evaluated between 20 and 5120 Hz and found to be of the type $1/f$. Mean values of the potassium, sodium, and leakage currents $\bar{I}_K$, $\bar{I}_{Na}$, and $\bar{I}_L$ were also measured by usual voltage-clamp techniques. Comparisons between these two types of data recorded under a number of different experimental conditions, such as presence of tetrodotoxin (TTX), substitution of calcium by lanthanum, and changes in the external concentration of potassium, have strongly suggested that the intensity of the fluctuations is related to the magnitude of $\bar{I}_K$.

INTRODUCTION

Instances where the available experimental techniques have been capable of detecting membrane "noise" directly are relatively rare. They include fluctuations in postsynaptic potentials (e.g. in cat motoneurons, Calvin and Stevens, 1968), in generator potentials of receptors (e.g. in *Limulus* eccentric cells, Dodge, Knight, and Toyoda, 1968), and in the axonal membrane (discussed below). The study of fluctuations is of importance because of the possible limitations or special characteristics (e.g. bounds on information rate in nerve channels, Stein, 1967, and linearizing of transfer functions as recently discussed by Spekereijse and Oosting, 1970) they may introduce in the signal transmission properties of neural structures. In addition, they can provide information about the intimate mechanism of these structures which is unavailable otherwise. The present paper is concerned with measurements of fluctuations of membrane current recorded in a voltage-clamped patch of lobster axon.

Measurements of the excitability of neural membrane have shown that the process of nerve impulse generation is not purely deterministic. In myelinated and unmyelinated axons, it is known that the response to a sequence of identical stimuli of threshold intensity is probabilistic: action potentials occur for only a fraction of the stimuli and the latency of the action potentials fluctuates randomly (Pécher,

1937; Verveen, 1961, 1962; Debecker, 1964; Poussart, 1966). Similarly, the interspike intervals recorded in the pacemaker cells of *Aplysia* in the absence of visible synaptic input are irregular (Junge and Moore, 1966).

Random fluctuations in the resting potential of axonal membrane were first reported by Verveen and Derksen (1965) for the frog node of Ranvier. These fluctuations, recorded under current clamp, had a power density spectrum which was inversely proportional to frequency over the range of 1 Hz–2 kHz. Their amplitude appeared to have a gaussian distribution with a standard deviation considerably larger than would be expected from the equivalent Johnson noise of the preparation. Hyperpolarization or depolarization by means of a constant current or changes in the external potassium concentration produced changes in the intensity of the fluctuations suggestive of a direct connection with the transport of potassium ions across the membrane. Verveen and Derksen also occasionally observed fluctuations in the form of small pulses of potential, somewhat resembling miniature end-plate potentials in shape, amplitude, and duration, and occurring in irregular bursts, usually for hyperpolarized values of membrane potential. The origin of this second and apparently distinct type of fluctuation is still uncertain although some of the data suggest a relationship with the diffusion of sodium (Verveen and Derksen, 1968, 1969).

In the present experiments, the fluctuations of the steady-state membrane current were recorded under voltage clamp. It has thus been possible to obtain further data on the nature of membrane fluctuations and on their relationship to known membrane processes. A short report summarizing this work has been published elsewhere (Poussart, 1969).

METHODS

The present study was conducted on single giant axons from the circumesophageal connectives of *Homarus americanus*. For our purposes, it will be convenient to consider the total membrane current I_m recorded under voltage clamp as the sum of a mean, net component $\bar{I}_m$ and of random deviations ΔI_m whose statistics we wish to study as a function of various experimental variables.

For convenience and for technical reasons (explained in the Appendix), we used two different voltage-clamp systems which could be connected interchangeably to the preparation, as shown in Fig. 1.

A first system, labeled "slow"-clamp system, was optimized for low noise operation with source resistances typical of a lobster node (e.g. 200 kΩ–1 MΩ). It recorded I_m while the membrane potential V_m was clamped to a slow linear ramp (rates, 0–±20 mv/sec). This system consisted of a field effect transistor headstage (2N4360, [Fairchild Semiconductor Div., Fairchild Camera & Instrument Corp., Hicksville, N.Y.] selected for low noise) followed by an operational amplifier (P45, [Philbrick/Nexus Researches, Boston, Mass.]). Its output was fed back to the preparation through a resistance of 10 MΩ (labeled r_f in the Appendix), a value which yielded a satisfactory compromise between low over-all instrumentation noise and adequate supply of current for clamping the node over the entire physiological range of V_m. The fluctuations ΔI_m were obtained by filtering out the slow component $\bar{I}_m$ (time con-

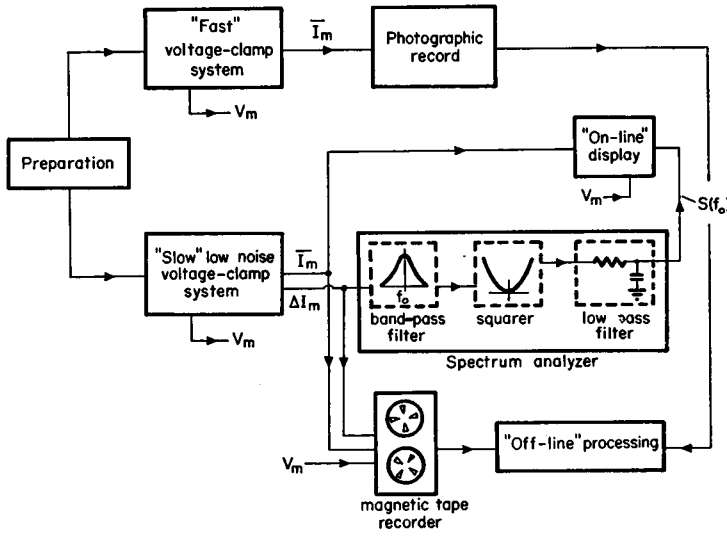

FIGURE 1 Block diagram of the experimental system. The preparation could be interchangeably connected to a "fast" voltage-clamp system for gathering conventional step-clamp data and to a "slow" voltage-clamp system, optimized for low noise operation and used for measuring the steady-state fluctuations of membrane current ΔI_m.

stant, 0.5 sec). Measurements on a passive electrical analogue of the preparation showed that the spot noise figure of this system ranged from 0.2 db at 5 kHz to 1 db at 50 Hz. The mean membrane current $\bar{I}_m$ and the power density spectrum $S(f)$ of ΔI_m in a particular frequency band (usually centered around 320 or 640 Hz) were displayed on-line as a function of V_m on a dual beam oscilloscope. $\bar{I}_m$, ΔI_m, and V_m were also recorded on FM magnetic tape (bandwidth, 0–10 kHz). $S(f)$ was measured for several frequencies off-line, by means of a bank of active filters with constant relative bandwidths (second order, $Q = 10$) whose squared outputs were averaged over appropriate periods of time. Measurements of $S(f)$ did not extend below 10 Hz because of the difficulties of maintaining the preparation in a "stationary" state over the longer averaging times required to obtain reliable estimates. Measurements of $S(f)$ were also limited to frequencies below 5 kHz by noise sources presumably not arising from the membrane (see Appendix).

A second, conventional, voltage-clamp system with fast rise time was used to obtain step-clamp data which were photographically recorded. The mean membrane current $\bar{I}_m$ flowing in response to a step change of V_m was then decomposed into the well-known peak "early" (sodium) $\bar{I}_{Na}$, "late" (potassium) $\bar{I}_K$, and unspecific "leakage" $\bar{I}_L$, currents (Blaustein and Goldman, 1966).

The preparation was placed in a Plexiglas chamber which followed the design of Julian, Moore, and Goldman (1962 *a*) with some modifications. The lengths of the sucrose gaps were kept to less than 1 mm to minimize the Johnson noise generated by the segment of axoplasm used as part of the voltage electrode. The central channel of the chamber, in which the artificial node is formed, was totally enclosed. This eliminated unevenness in the flow of the test solution which may arise in an open channel because of surface tension effects. It also provided smooth control of the width of the node. Any one of four test solutions could be selected by means of a miniature distribution valve. A change of solutions could be com-

pleted in a few seconds because of the small volume of the chamber. Electrical connections to the chamber were made though KCl agar bridges and Ag-AgCl electrodes.

The solutions used included isotonic sucrose (725 mM $C_{12}H_{22}O_{11}$), artificial seawater (ASW: 465 mM NaCl, 10 mM KCl, 4 mM $MgCl_2$, 4 mM $MgSO_4$, 25 mM $CaCl_2$), lanthanum seawater (LaSW: 457 mM NaCl, 10 mM KCl, 4 mM $MgCl_2$, 4 mM $MgSO_4$, 15 mM $LaCl_3$) and isotonic potassium chloride (KCl: 478 mM KCl, 4 mM $MgCl_2$, 4 mM $MgSO_4$, 25 mM $CaCl_2$). Changes in external potassium concentration were achieved by mixing appropriate amounts of ASW and KCl. The test solutions were unbuffered. A microthermistor mounted in the central channel continuously monitored the temperature which ranged between 6 and 9°C.

For a typical experiment, a node was first tested for resting potential and ability to respond to stimulation by an action potential. V_m was then swept through its physiological range (usually twice, for later averaging) and both $\bar{I}_m$ and ΔI_m were measured by the "slow"-clamp system. A set of step-clamp data were next obtained using the "fast"-clamp system. Switching between the two systems was automated so that one complete sequence of noise and step-clamp data could be performed in approximately 2 min. The process was then repeated with a different test solution and again with the original test solution.[1]

RESULTS

Measurements in ASW

Spectral Characterization. In Fig. 2 the filtered mean square values of the fluctuations ΔI_m are shown as a function of V_m for a typical node bathed in ASW. Two observations can be made.

(*a*) For any given V_m, the outputs of all filters with center frequencies f_0 between 20 Hz and 1.28 kHz are approximately the same. Since the filters have bandwidths proportional to f_0, this indicates that the power density spectrum $S(f)$ of ΔI_m is inversely related to frequency.

(*b*) The energy in ΔI_m is a function of V_m.

These data may be replotted with V_m as a parameter in order to yield power density spectra, as shown in Fig. 3 for a different preparation.

For frequencies between 20 Hz and approximatively 600 Hz for negative values of V_m and up to 2 kHz for large positive values of V_m, $S(f)$ decreases with increasing frequency.

For frequencies above this range, $S(f)$ becomes flat or increases in magnitude with frequency, and becomes progressively less dependent upon V_m. This behavior is believed to result from an artifact. Control measurements performed on a passive equivalent circuit of the preparation, shown as the lower (solid) curve, and theoretical arguments developed in the Appendix support this interpretation of the data. As predicted by equation A 4 and confirmed by these control measurements, the membrane capacity brings about an effective increase of the contribution of instrumentation noise (amplifier plus Johnson noise of voltage electrode) to the

[1] The dimensions of the node were not accurately measured. Variations in nodal areas through a series of solution changes were minimized by carefully equalizing the head of hydrostatic pressure of the various test solutions.

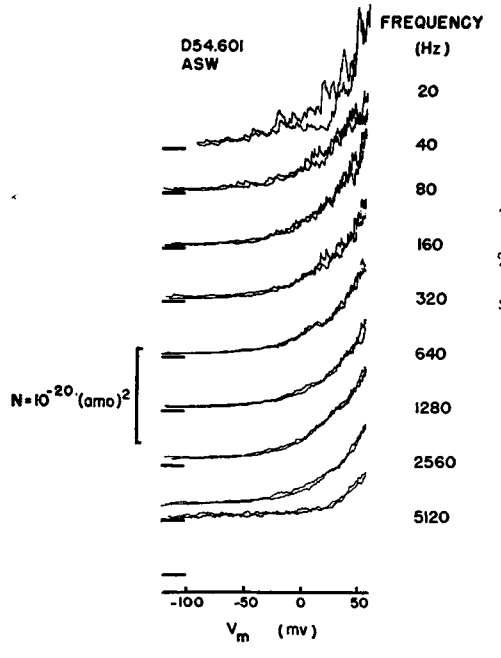

Figure 2

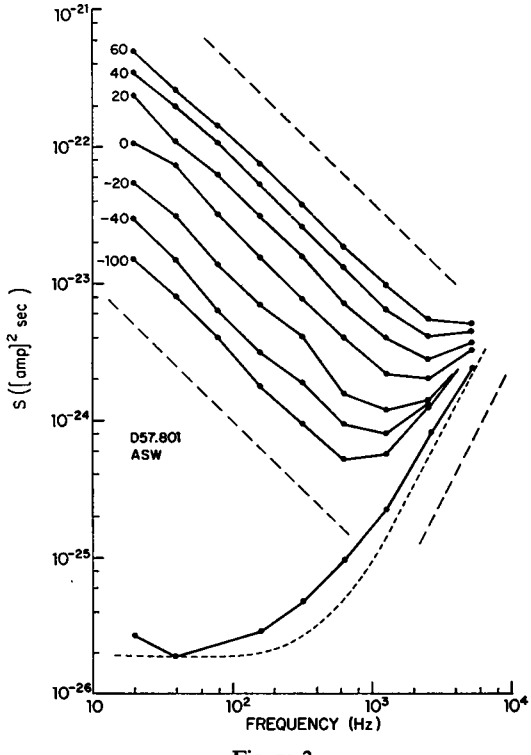

Figure 3

FIGURE 2 Mean square value of the fluctuations of steady-state membrane current in the passbands of a set of filters. The center frequencies of the filters are indicated in the right-hand column and the baseline for each tracing is indicated by the heavy bar on the left-hand side of each tracing. The figure shows data obtained for two successive sweeps of V_m with a clamping potential consisting of a ramp with a slope of 2 mv/sec.

FIGURE 3 Upper family of curves: power density spectra, $S(f)$, (plotted in log-log coordinates) of fluctuations of membrane current recorded in a node bathed in ASW for clamped membrane potentials ranging from -100 to $+60$ mv. The dashed lines have slopes of -1 and $+2$.

Lower curves: Theoretical spectrum for a noiseless amplifier (dashed curve) and measurements (solid curve), respectively, of the current noise recorded on a passive electrical equivalent circuit of a preparation with membrane resistance r_m of 1 MΩ, membrane capacity c_m of 910 pF, and axoplasm resistances of 150 kΩ.

recorded noise, with an asymptotic rate of 20 db/decade of frequency. The high frequency portions of the spectra measured on the preparation are in close agreement with the predicted values based upon this artifact, both in absolute value and in frequency dependence. All of the forthcoming discussions of membrane noise refer to the low frequency portion of the data for which this extraneous noise contribution can be neglected.

The set of relatively straight and parallel lines on these log-log coordinates suggests that, in the region of interest, the data can be fit by a power-law expression of

the form

$$S(f) = Nf^{-a} \tag{1}$$

where N is some function of V_m and a is a dimensionless quantity. The values of a determined on 250 spectra from 22 nodes in ASW[2] were found to have a uninodal distribution, with a range of 0.8–1.3, a mean of 1.002, and a standard deviation of 0.076. No systematic dependence between a and V_m was apparent. It seems appropriate, therefore, to characterize the spectrum of ΔI_m as of the kind $1/f$ over the full range of V_m :

$$S(f) = Nf^{-1}. \tag{2}$$

Dependence of N on V_m . Figs. 2 and 3 have also shown that the fluctuations ΔI_m become more intense as V_m is increased towards positive values (depolarized). In Fig. 4, this effect is shown more explicitly in a plot of N vs. V_m (filled circles). For this node in ASW, N is approximately constant for V_m extending from -100 to -50 mv. As V_m is further increased, N increases, typically reaching a 30- to 40-fold increase at $+60$ mv. Although barely visible in the figure, there is a poorly defined minimum of N which is frequently detectable for V_m between -70 and -90 mv. This last point is discussed further later.

The plot of N vs. V_m shown in Fig. 4 is similar to data obtained on more than 100 nodes. However, a considerable scatter (of more than one order of magnitude) was noted in the absolute values of N measured on different nodes for the same V_m . This dispersion may reflect differences in the nodal areas plus normal variations in the membrane characteristics of different preparations.

Correlation between N and $\bar{I}_K$; Measurements with Tetrodotoxin. A simulation of the Hodgkin-Huxley equations for the squid axon on a hybrid computer (Demko, 1968) showed that for a ramp clamp such as used in these experiments, the peak early (sodium) current $\bar{I}_{Na}$ remains essentially inactivated while the late (potassium) current $\bar{I}_K$ assumes its "steady-state" value for slopes of ramp voltage up to 20 mv/sec. Ramp clamps of varying slopes have been used by others (Fishman and Macey, 1969) to measure the different ionic currents in frog skin. It is known that the late current recorded under step-clamp conditions in the lobster axon shows no inactivation (Julian, Moore, and Goldman, 1962 *b*). Except for a small hysteresis effect which occurs when the direction of the ramp clamp is reversed, there was no discrepancy between the values of $\bar{I}_m$ measured 10 msec after the onset of a step clamp and those recorded in a continuous fashion under a ramp clamp. Hence it has been assumed that $\bar{I}_m$ flowing during the noise measurements could be resolved into potassium and leakage components according to the step-clamp data obtained on the same node.

[2] For consistency, and because it is an unbiased estimate, the straight line of "best fit" was operationally defined as that passing through the mid points of the segments joining $S(40)$ and $S(80)$, and the segment joining $S(320)$ and $S(640)$, for a given V_m .

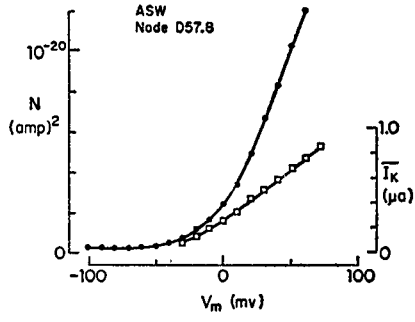

FIGURE 4 Filled circles: plot of N as a function of V_m. Open squares: plot of the steady-state potassium current $\bar{I}_K$ also as a function of V_m. These two sets of data are recorded from the same node in ASW.

TTX was used in order to further test whether the early channel was in fact inactivated during a ramp clamp and to examine whether TTX has any measurable effect on the noise current ΔI_m. In a step clamp, TTX is known to selectively suppress the early current when applied externally while leaving the characteristics of the late and leakage currents unchanged (Narahashi, Moore, and Scott, 1964; Takata, Moore, Kao, and Fuhram, 1966). TTX also blocks the small component of the early current which is carried by potassium (Chandler and Meves, 1965; Rojas and Atwater, 1967).

In our experiments, the addition of 200 nM TTX to ASW (ASW + TTX), bathing the preparation, suppressed excitability and the early component of current in response to a step clamp within 1 min of its application. No significant changes could be detected in the fluctuation ΔI_m recorded on the same node in ASW and in ASW + TTX. As illustrated in Fig. 5, the application of TTX did not modify the general form of $S(f)$ which could again be written as Nf^{-a} with a taking values close to 1. Small differences in the absolute level of $S(f)$ for given V_m were occasionally noted (see Fig. 7). These differences were not systematic and could plausibly be explained by small changes in the area of the node following a change in the solution. From these data, it appears rather unlikely that the steady-state fluctuations can be related to the flow of ions through the early channel.

The dependence of the intensity of the fluctuations, N, on membrane potential, V_m, measured in ASW bears a qualitative similarity to the mean, net "steady-state" potassium current $\bar{I}_K$ obtained from step-clamp data (see Fig. 4, open squares). Precise estimates of $\bar{I}_K$ are difficult to obtain for V_m less than approximately -40 mv because of the relatively large contribution of the unspecific leakage component, $\bar{I}_L$, to the total membrane current and because it is difficult to separate $\bar{I}_L$ from $\bar{I}_K$.[3] Measurements of $\bar{I}_L$ by the simultaneous application of external TTX and internal tetraethylammonium have not yet been reported for lobster axons. Nevertheless, it is apparent from the data of Fig. 4 that N increases significantly for the

[3] For example, in the vicinity of resting potential the Hodgkin-Huxley model for squid axon yields values of the leakage and steady-state potassium conductances, g_L and g_K, which are comparable, 0.3 and 0.36 mmho/cm^2, respectively.

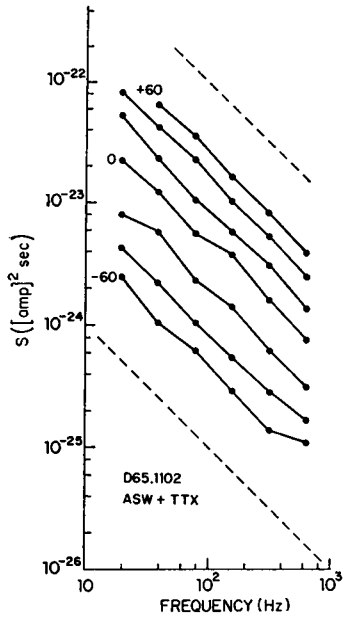

FIGURE 5 Power density spectra, $S(f)$, (plotted in log-log coordinates) recorded in ASW + TTX for membrane potentials ranging from −60 to +60 mv in increments of 20 mv. The straight dashed lines have slopes of −1.

same range of values of V_m for which $\bar{I}_K$ becomes appreciable, and that both N and $\bar{I}_K$ increase monotonically with V_m beyond that region.

These observations are consistent with the hypothesis that the current fluctuations measured in ASW are related to the potassium system, in particular to the flow of potassium ions. The relation between N and $\bar{I}_K$ is shown in Fig. 6 for a node in ASW. Comparable data were secured on 17 nodes. Without exception, it was found that these data could be fit by a function of the form

$$N = A + B(\bar{I}_K), \tag{3}$$

where A is a positive constant independent of V_m and $\bar{I}_K$, and $B(\bar{I}_K)$ is a positive, monotonically increasing function of $\bar{I}_K$. The constant A will be discussed later.

The relationship between B and $\bar{I}_K$ can be fit by means of a power law,

$$B(\bar{I}_K) = k\bar{I}_K^m \tag{4}$$

as shown in Fig. 7 (open circles) where k and m are parameters that are independent of V_m and $\bar{I}_K$. For these data, V_m is greater than −50 mv for the reasons mentioned above. This figure is an example of a node for which data was available over a particularly wide dynamic range of B and $\bar{I}_K$, and where a power law with $m = 2.1$ appears to hold over more than a 100-fold variation of B. Data for this node bathed in ASW + TTX are also shown in Fig. 7 (filled circles). TTX does not modify the relationship between B and $\bar{I}_K$. The value of m was determined for 17 nodes and ranged between 1.1 and 2.1 with a mean of 1.5.

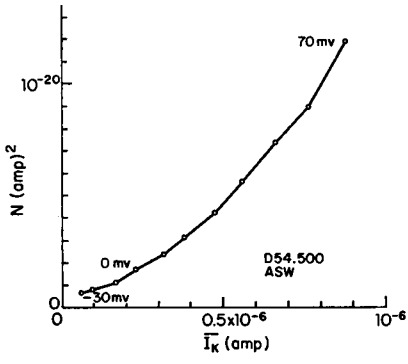

Figure 6

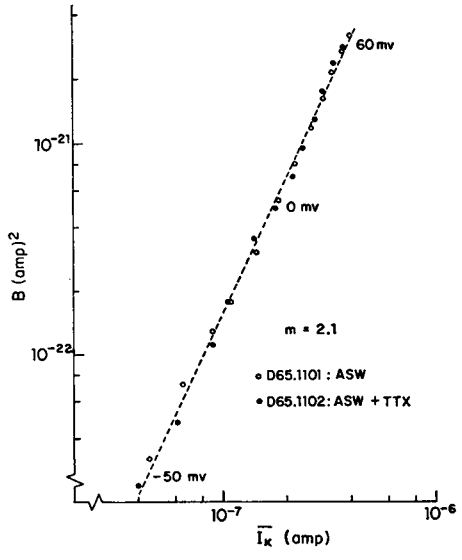

Figure 7

FIGURE 6 N as a function of the potassium current $\bar{I}_K$ measured for values of V_m ranging from -30 to $+70$ mv in increments of 10 mv. For each value of V_m, N and $\bar{I}_K$ were measured and are plotted in linear coordinates. Node D54.500 in ASW.

FIGURE 7 Relation between B and $\bar{I}_K$ in the expression $N = A + B(\bar{I}_K)$ for V_m ranging from -50 to $+60$ mv in increments of 10 mv. Data recorded in ASW (open circles) and in ASW + TTX (filled circles).

We have already noted the dependence of N upon V_m. The above data, however, suggest that this dependence is probably not direct, but may only exist through the quantity $\bar{I}_K$. Further support for this interpretation comes from pooling the results obtained on several nodes.

In order to pool the data in a meaningful manner, it is necessary to compensate in some way for differences in the areas of the nodes in different experiments. Note, for example, that doubling $\bar{I}_K$ by depolarizing the membrane typically increases B approximately fourfold (see Fig. 7). It is reasonable to assume, however, that doubling $\bar{I}_K$ by doubling the area of the nodal membrane, while keeping V_m constant, would double B.[4]

Since we did not determine the area of each node accurately, the following procedure was used to normalize the data. For a given node, the measured values of B and $\bar{I}_K$ were both multiplied by a constant which was defined as the ratio of the value of $\bar{I}_K$ measured on a reference ("typical") node to that measured on the given node for $V_m = 10$ mv. This value of V_m was chosen because it lies approximately mid-range in the plot of $\bar{I}_K$ vs. V_m. Node D57.800 was chosen as the reference. The

[4] We are assuming that the nodal membrane has uniform spatial characteristics and that the dimensions of the node are much larger than the distance over which the individual sources of membrane current fluctuations are correlated. No data are presently available to confirm or deny this assumption.

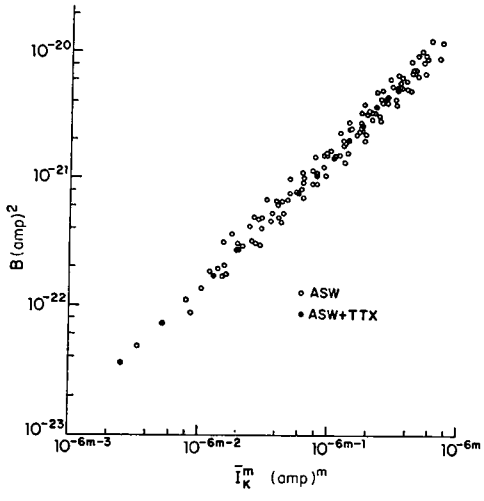

FIGURE 8 Relation between B and $\bar{I}_K^m$ measured on 17 nodes in ASW (open circles) and 1 node in ASW + TTX (filled circles) for V_m ranging from -50 to $+70$ mv. These data are corrected for the "area" of the nodes according to the procedure described in the text.

constant computed in this manner ranged from 0.4 to 1.5 on this population of 17 nodes.

The results are shown in Fig. 8 in a plot of the corrected values of B vs. $\bar{I}_K^m$ with the individually determined values of m used for each node. It is significant that for all values of $\bar{I}_K^m$ obtained on these 17 axons, the range of the scatter of B is only of the order of 2–1 and is considerably smaller than the dispersion of the values of B corresponding to a particular value of V_m. Moreover, we note that pooling of data from these 17 axons in ASW extends the range of B for which the relationship

$$B = k\bar{I}_K^m$$

appears to hold to more than two and one-half decades. These data yield a value of k of 1.41×10^{-20} (amp)^2 sec/μa^m for a "typical" lobster node in ASW with an area estimated to be $1.5 \times 10^4\ \mu^2$.

Relation of Fluctuations to Leakage Current. A scattergram of values of N vs. the leakage current $\bar{I}_L$ constructed from data obtained on 17 axons in ASW, 1 axon in ASW + TTX, and 3 axons in LaSW (discussed below) at $V_m = 10$ mv, has shown no visible trend, even following corrections to account for nodal "area," as described above. Thus it would appear that the bulk of ΔI_m is unrelated to the flow of the leakage current $\bar{I}_L$. However, in view of the somewhat operational definition of $\bar{I}_L$, the existence of a relationship between some components of ΔI_m and $\bar{I}_L$ cannot be entirely ruled out.

Measurements following Changes in the Potassium System

It has been shown that the measured power density spectrum $S(f)$ of the fluctuations of steady-state membrane current for an axon in ASW could be fit empirically

by the equation:

$$S(f) = \frac{A + k\bar{I}_K^m}{f^a}, \tag{5}$$

where A, k, m, and a are parameters that are independent of membrane potential and $\bar{I}_K$ is the net (outward) potassium current.

According to the Hodgkin-Huxley model of neural membrane, $\bar{I}_K$ is given by the expression

$$\bar{I}_K = g_K(V_m - E_K), \tag{6}$$

where g_K is the potassium conductance and E_K is the Nernst equilibrium potential of potassium,

$$E_K(\text{mv}) = 57 \log_{10} \frac{[K]_o}{[K]_i}, \tag{7}$$

where $[K]_o$ and $[K]_i$ denote the external and internal concentrations of potassium, respectively. In the lobster axon, $[K]_i$ range from 200 to 300 mM (Brinley, 1965). Experiments were conducted to determine whether conditions known to change the parameters of the potassium system (either E_K or g_K) would change the fluctuations of membrane current in a predictable manner.

Effect of Changes in g_K Induced by Lanthanum. For the lobster axon, the substitution of lanthanum for the calcium normally present in ASW (LaSW) is known to reduce the peak sodium and steady-state potassium conductances while increasing their activation times. The leakage conductance is also decreased (Takata, Pickard, Lettvin, and Moore, 1966). The external application of lanthanum parallels, although more potently, the effects obtained on various preparations by increasing the calcium concentration beyond its normal value of 25 mM (Frankenhaeuser, 1957; Frankenhaeuser and Hodgkin, 1957; Blaustein and Goldman, 1966).

More specifically with regards to the potassium system, the application of 15 mM La is followed by a gradual shift along the V_m axis of the curve relating $\bar{I}_K$ to V_m. The shift typically reaches +25 to +35 mv after 1–3 min. Following this initial phase, during which the action of lanthanum is reversible, a second irreversible phase develops, during which a slight additional shift occurs and the slope of the $\bar{I}_K$-V_m curve decreases (Takata, Pickard, et al., 1966).

Comparative measurements of the fluctuations ΔI_m in ASW and LaSW were made on more than 60 nodes and full spectral analysis performed on 7 nodes. Fig. 9 shows two typical spectra $S(f)$ measured on the same node in ASW and following 2.5 min perfusion in LaSW. We first note that the frequency dependence of $S(f)$ in LaSW remains the same as in ASW: the spectra are of the form f^{-a}, with a close to 1.0 (this has been confirmed for 75 individual spectra). The reduction of N in

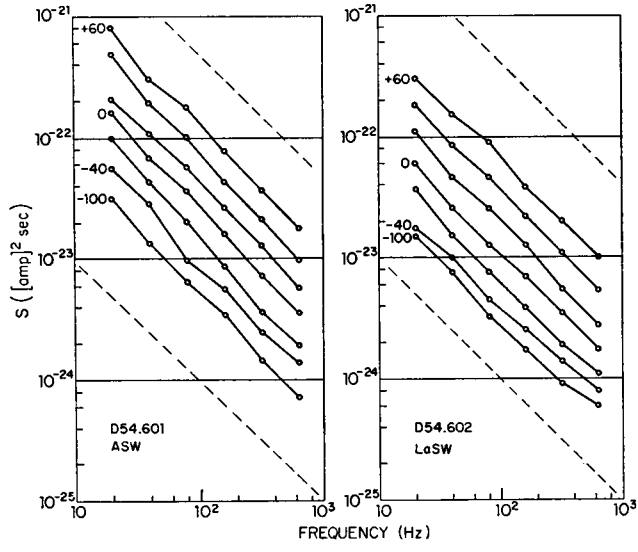

FIGURE 9 Power density spectra, $S(f)$, measured in ASW (left) and in LaSW (right) on the same node, for V_m ranging from -100 to $+60$ mv. The dashed lines have slopes of -1.

LaSW, which is visible in Fig. 9, is shown more explicitly in Fig. 10. Similar results were obtained on all nodes investigated. Qualitatively, the effect of LaSW on the relation between N and V_m appears to be similar to its effect upon the relation between $\bar{I}_K$ and V_m. To a first approximation, the changes in N can also be described as a simple shift of the N vs. V_m relation of about $+30$ mv. As shown in the figure, the action of LaSW on N is reversible (during the initial phase of application) as its known effect on $\bar{I}_K$.

Unfortunately, the action of lanthanum develops slowly and the characteristics of the membrane still undergo changes after 10 min of continuous perfusion in LaSW. Significant changes could occur during the period of time required to obtain a full set of noise and step-clamp measurements. For this reason, we have not attempted to correlate N and $\bar{I}_K$ quantitatively in LaSW.

Effects of Changes in E_K. In ASW, with $[K]_o = 10$ mM, equation 7 predicts a corresponding E_K of approximately -80 mv. The relatively large contribution of the leakage system, which was noted before, makes it difficult to determine the value of V_m for which $\bar{I}_K$ is zero. Only positive (outward) potassium currents can be easily and reliably measured. However, by increasing $[K]_o$, hence E_K, negative (inward) potassium currents of appreciable magnitude can be made to flow through the nodal membrane (Moore, 1959; Julian et al. 1962 *b*).

Experiments were conducted in order to determine whether equation 5, which was derived for positive $\bar{I}_K$, could be extrapolated to the region of negative $\bar{I}_K$

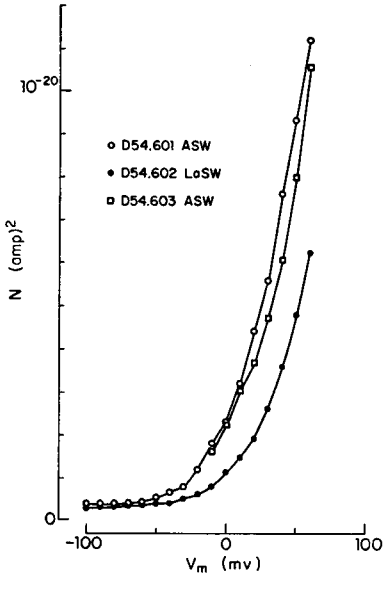

FIGURE 10 Plot of the intensity of the fluctuation N as a function of V_m, measured in ASW (open circles), then following a perfusion of 2.5 min in LaSW (filled circles), and after the reapplication of ASW (open squares).

by the simple modification

$$S(f) = \frac{A + k|\bar{I}_K|^m}{f^a}, \tag{8}$$

or whether an altogether different expression for $S(f)$ would be required.

This conjecture was assessed by examining (*a*) whether the spectral density of the fluctuations recorded with various $[K]_o$ remained of the f^{-a} type, (*b*) whether the minimum in the intensity of the fluctuations predicted by equations 6 and 8 for $\bar{I}_K = 0$ (i.e. at $V_m = E_K$) could be observed, and (*c*) whether the intensity of the fluctuations was related to the magnitude of $\bar{I}_K$ in the form shown in equation 8.

Fluctuations of membrane current ΔI_m were recorded on more than 50 nodes with $[K]_o$ equal to 81, 244, and 478 mM, and spectral analysis was performed on 19 of these nodes. Fig. 11 shows a typical family of power density spectra $S(f)$ measured with $[K]_o$ = 244 mM. Because the dependence of the intensity on V_m is not monotonic, the data are plotted in three dimensions.

The figure shows that $S(f)$ is inversely related to frequency over the range of 20 Hz–1 kHz or more, independent of V_m. A similar frequency dependence occurred for all nodes bathed in solutions of high potassium concentration. Values of a measured on 183 spectra with $[K]_o$ equal to 81, 244, and 478 mM were similar to those measured in ASW and did not show any obvious dependence on V_m and/or on $[K]_o$. It appears, therefore, that the $1/f$ character of the spectra is insensitive to V_m and $[K]_o$.

Equations 6–8 predict that the dependence of the intensity of the fluctuations on

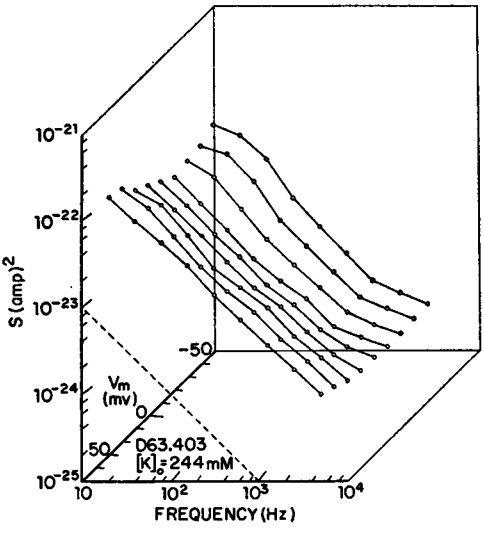

Figure 11

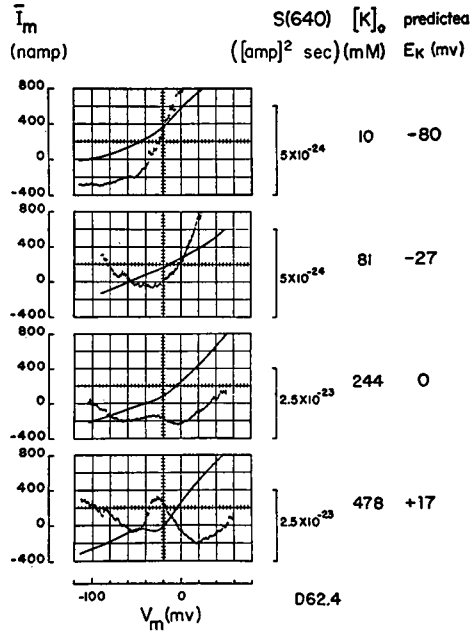

Figure 12

FIGURE 11 Power density spectra $S(f)$ vs. f and V_m. Data recorded from a node in sea water whose potassium concentration $[K]_o$ was 244 mM. V_m ranged from -30 to $+50$ mv increments of 10 mv. The dashed line has a slope of -1 in these log-log coordinates.

FIGURE 12 On-line measurements of the power density spectrum of the fluctuations at 640 Hz, $S(640)$, and of the total membrane current $\bar{I}_m$ as a function of V_m. Data recorded from node D62.4 with a $[K]_o$ of 10, 81, 244, and 478 mM. Note that the lowest minimum in $S(640)$ shifts toward more positive V_m as $[K]_o$ is increased. This particular node exhibited a region of negative slope conductance for $[K]_o$ = 478 mM (and possibly for $[K]_o$ = 244 mM).

the membrane potential, V_m, will change as E_K is changed by altering $[K]_o$. In particular, the curve of N vs. V_m should have a minimum for $\bar{I}_K = 0$, at $V_m = E_K$.

The general nature of the effects produced on the intensity of the fluctuations for different $[K]_o$ is illustrated in Fig. 12 as an example of the on-line display of the data which was routinely performed in these experiments. It shows measurements of $S(640)$ and of $\bar{I}_m$ plotted vs. V_m, obtained for one node for values of $[K]_o$ of 10, 81, 244, and 478 mM. These data represent but a fraction of the complete set of measurements typically performed on one node. Experiments in which the concentrations were varied usually were repeated for various sequences of concentrations and verified the reversibility of the results.

It is apparent in the data of Fig. 12 that there exist certain ranges of V_m for which the intensity of the fluctuations reaches an absolute minimum level. For $[K]_o$ = 10 mM (ASW) the intensity of the fluctuations exhibits a very broad, poorly defined minimum in the range of V_m of -70 to -100 mv (as was mentioned previously).

A proper minimum could frequently be observed in this range, provided the data were processed with a sufficiently large gain. This was not done routinely because the intensity of the fluctuations then generally exceeded the dynamic range of the instrumentation for more positive values of V_m. Measurements of $S(320)$ for two different scales on a node in ASW, shown in Fig. 13, illustrate an example of such a minimum. Note that the minimum occurs at membrane potentials of approximately -85 mv which coincides closely with the value of E_K of approximately -80 mv predicted by equation 7.

For $[K]_o = 81$ mM, the plot of the on-line estimate of $S(640)$ vs. V_m shown in Fig. 12 exhibits a minimum between -20 and -40 mv. This compares closely with the value of E_K of approximately -27 mv predicted for this external concentration of potassium.

Similarly, for $[K]_o = 244$ mM, the intensity of the fluctuations reaches an absolute minimum for membrane potentials which are close to the predicted value of E_K of approximately 0 mv. In this case, however, a local minimum also occurs in the curve for $V_m = -60$ mv. It is believed that this second minimum is related to the steady-state negative slope conductance of potassium which is obtained over a certain range of V_m for high external concentration of potassium (Julian et al., 1962 *b*). This second minimum has rarely been observed at an external concentration of potassium of 244 mM but was frequently observed at the higher $[K]_o$ of 478 mM (see below).

For $[K]_o = 478$ mM, a minimum of the intensity occurs for more positive values of V_m, at approximately $+20$ mv. The value of E_K predicted on the basis of equation 7 is $+17$ mv. Again, a second local minimum of the intensity of the fluctuations occurs at more negative values of V_m. It will be suggested below that the lower minimum corresponds to the point where $\bar{I}_K = 0$ while the other minimum corresponds to a local minimum of the magnitude of $\bar{I}_K$.

From these illustrative examples, it is apparent that the intensity of the fluctuations of steady-state membrane current reaches a minimum when V_m lies in the region of E_K., i.e. when $\bar{I}_K$ is presumably small. These results, and those of other similar experiments, have been pooled. The quantity $V_{m,min}$ is defined as the membrane

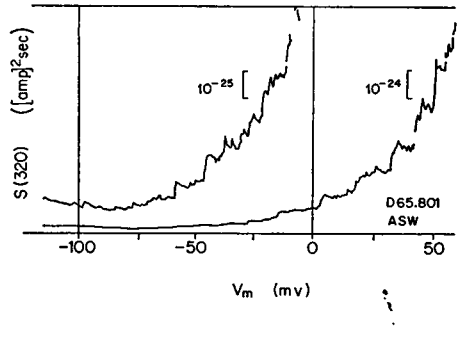

FIGURE 13 Examples of minima in the intensity of the fluctuations vs. V_m for nodes in ASW. Intensity of the fluctuations on the same node for two different scales measured at 320 Hz. A broad minimum can be seen for the data plotted with higher resolution.

potential for which the intensity of the fluctuations is a (lowest) minimum. Because of the difficulty of defining $V_{m,\min}$ from plots of N vs. V_m, the following procedure has been arbitrarily selected. For a given node at a given $[K]_o$, the membrane potentials corresponding to the absolute minima of the intensities of the fluctuations in each of the passbands of the analyzing filters were measured and the average of these measurements was defined as $V_{m,\min}$.

Fig. 14 shows a plot of $V_{m,\min}$ vs. E_K for 30 recordings on 18 nodes from 7 axons. Clearly the membrane potentials corresponding to the minima are highly correlated with E_K. The dispersion of points about the line may be accounted for by such factors as the statistical errors in the estimates of $V_{m,\min}$, the variations in $[K]_i$ which are known to occur from axon to axon (Brinley, 1965), and the residual potential of a few millivolts which can exist across the axonal membrane depolarized by the solution of isotonic KCl ("V pool") and which appears in series with V_m (Julian et al., 1962 *a*).

Measurements in an external potassium concentration of 478 mM are of particular interest because: (*a*) for this value of $[K]_o$ a negative $\bar{I}_K$ of appreciable magnitude can flow through the nodal membrane, and (*b*) the steady-state V_m-$\bar{I}_K$ characteristics of the membrane frequently exhibit a region of negative slope conductance. It is

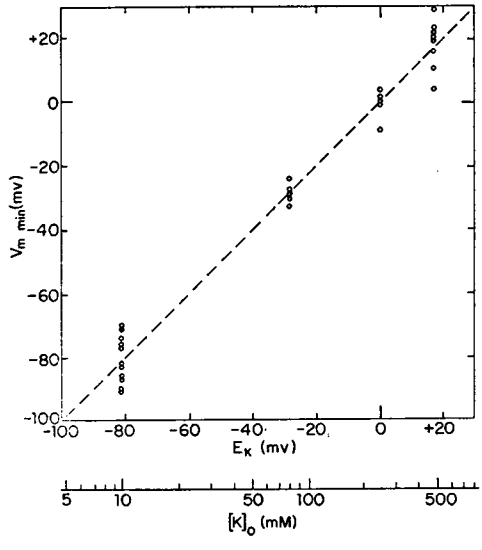

Figure 14

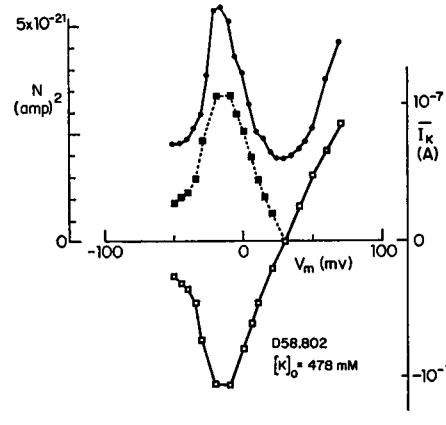

Figure 15

FIGURE 14 Scattergram of $V_{m,\min}$ vs. the external potassium concentration $[K]_o$ and the corresponding equilibrium potential E_K. Data gathered on 18 nodes obtained on 7 axons.

FIGURE 15 Filled circles: plot of N as a function of V_m measured in a node which exhibited negative slope conductance in high $[K]_o$. Open squares: corresponding net potassium current $\bar{I}_K$ derived from step-clamp measurements. Filled squares: absolute value of potassium current $\bar{I}_K$, for portion of $\bar{I}_K$ vs. V_m that is negative (inward).

thus possible to obtain identical values of $\bar{I}_K$ for two or more values of membrane potential.

Steady-state V_m-$\bar{I}_K$ characteristics with a region of negative slope conductance have been observed in high $[K]_o$ in a number of preparations including the node of Ranvier (Mueller, 1958), the giant axon of the squid (Moore, 1959; Ehrenstein and Gilbert, 1966; Lecar, Ehrenstein, Binstock, and Taylor, 1967), and the lobster giant axon used in our experiments (Julian et al., 1962 *b*).

Fig. 15 shows plots of the intensity of the fluctuations N and of the potassium current $\bar{I}_K$ recorded from a node which exhibited negative slope conductance. $\bar{I}_K$ is derived from step-clamp data, following correction for $\bar{I}_L$ (Lecar et al., 1967). $|\bar{I}_K|$ is also shown in this figure. It is clear that the dependence of N on V_m is qualitatively similar to the dependence of $\bar{I}_K$ on V_m.

We define, as previously, the quantity N as the sum of two terms

$$N = A + B(\bar{I}_K),$$

where

$$A = N|_{I_{K=0}}$$

and plot $B(\bar{I}_K)$ vs. $\bar{I}_K$ with V_m as a parameter (see Fig. 16). Experimental points corresponding to successive values of V_m are joined by straight lines. Note that the three monotonic portions of the graphs of N and of $|\bar{I}_K|$ vs. V_m of Fig. 15 seem to superimpose. Furthermore, on these log-log coordinates the data points generally fall around a straight line whose slope, 1.87, is not unlike that of similar plots obtained from nodes in ASW.

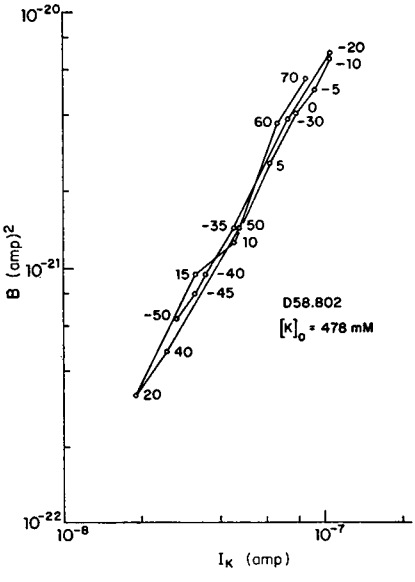

FIGURE 16 Plot, in log-log coordinates, of the quantity B as a function of the magnitude of the net potassium current with $[K]_o$ = 478 mM recorded for values of V_m ranging from −50 to +70 mv. Same data as shown in Fig. 15.

These data support the contention that the intensity of the fluctuations N is related directly to the magnitude of the mean, net, steady-state potassium current. The relation of N to V_m would appear to be indirect. For instance, several values of V_m (for example, -65, -43, -5 mv and $+50$ mv for $N = 1.25 \times 10^{-23}$ (amp)^2, for $[K]_o = 478$ mM in Fig. 12) can correspond to a single value of the intensity of the fluctuations. The same comment applies to g_K which is believed to be a monotonic function of V_m in high $[K]_o$, at least for the range of membrane potential used in our study (Moore, Anderson, Blaustein, Takata, Lettvin, Pickard, Bernstein, and Pooler, 1966; Lecar et al., 1967).

The above data are also of interest because they further demonstrate the validity of assigning the observed fluctuations to membrane processes. The artifact electrical noise produced by the clamping amplifier at a given frequency is dependent solely on the incremental impedance of the source (see Appendix). In high $[K]_o$ it is apparent, however, that quite different intensities of fluctuations can be observed for the same source resistance. For example Fig. 12, for $[K]_o = 478$ mM, shows that there exist two points, at $V_m = -45$ and -30 mv, where the membrane slope resistances are equal (and infinite) but the intensities of fluctuations are different. In fact, we note that the point $V_m = -45$ mv corresponds approximately to a local

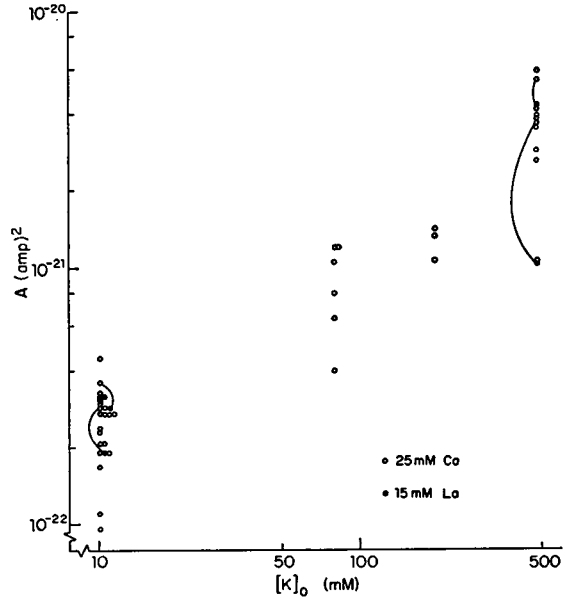

FIGURE 17 Scattergram of the quantity A which appears in the expression $N = A + B(\bar{I}_B)$, plotted (in log-log coordinates) vs. the external concentration of potassium (open circles). Data obtained on 41 nodes from 22 axons and not corrected for the "area" of the nodes. The figure also shows the changes in A resulting from the substitution of lanthanum for the calcium normally present in the test solution (filled circles).

minimum value of N while the point $V_m = -30$ mv corresponds to a local maximum of N.

Dependence of A on $[K]_o$. These data show that the minimum intensity of the observed fluctuations occurs approximately for $\bar{I}_K = 0$. For this value, $N = A$. We have examined the dependence of A on $[K]_o$.

A scattergram of values of A measured on 22 axons and plotted vs. $[K]_o$ is shown in Fig. 17. Because of the various concentrations of potassium used, it is not possible to normalize these data for differences in nodal area according to the procedure described before. It is not appropriate therefore to derive a quantitative relationship between A and $[K]_o$. However, A appears to increase with higher external concentrations of potassium. Fig. 17 also includes a few measurements obtained with lanthanum substituted for calcium in the test solution. These indicate that the presence of lanthanum also decreases the intensity of the fluctuations when $\bar{I}_K$ is zero.

DISCUSSION

The only other published reports of measurements of noise of axonal membrane are those of Derksen and Verveen (Derksen, 1965; Derksen and Verveen, 1966; Verveen and Derksen, 1965, 1968, 1969; Verveen, Derksen, and Schick, 1967). They reported measurements of the fluctuations of the steady-state potential of a node of Ranvier. Their results can be compared to ours in the following manner: because of the small amplitude of the fluctuations, it is reasonable to expect that for a given node with slope resistance r_m, the fluctuations of membrane current ΔI_m are related to the fluctuations of membrane potential ΔV_m by the relationship

$$\overline{\Delta I_m^2} = \frac{\overline{\Delta V_m^2}}{r_m^2}, \tag{9}$$

at least over the range of frequencies where the effects of the capacity of the membrane c_m can be neglected (e.g. below 400 Hz). For these frequencies, therefore, the spectral density of the current and of the voltage fluctuations can both be expected to have the same frequency dependence.

In the present study, the spectral density of the fluctuations was analyzed over a frequency range extending from 20 Hz up to 5 kHz and found to be of the form f^{-a}. The quantity a, which was determined for 433 individual spectra, was found to have a value close to 1, independent of membrane potential V_m, membrane current $\bar{I}_m$, and/or the external concentration of potassium $[K]_o$. These data are in substantial agreement with those of Derksen and Verveen. The spectra which they have measured in normal Ringer solution exhibit a similar frequency dependence: values of a which we have estimated on 18 of their spectra range from approximately 0.7 (Derksen, 1965, Fig. 3.3.3.-3) to 1.2 (Derksen, 1965, Fig. 3.2.1.-4) with a mean value close to 1.

Equation 9 can be used to compare the absolute levels of the intensity of the fluctuations recorded in a node of Ranvier and in a node simulated on the giant lobster axon. According to equation 9, and because of the gross similarities between the electrical characteristics of these two preparations, we might compare the quantity

$$\overline{\Delta I_m^2} \text{ (for the lobster node)}$$

to the quantity

$$\frac{\overline{\Delta V_m^2}}{r_{mR}^2}\left(\frac{r_{mR}}{r_{mL}}\right), \tag{10}$$

where r_{mR} and r_{mL} are the membrane resistances of a node of Ranvier and of a lobster node, respectively, and $\overline{\Delta V_m^2}$ is measured on the node of Ranvier. The scaling factor r_{mR}/r_{mL} is used to account for differences in the effective areas of the two types of nodes.[5] On this basis, absolute levels of the fluctuations recorded on the Ranvier node and on the lobster axon appear to have similar orders of magnitude. For example, for a typical lobster node of this study, e.g. node D54.8, the value of N measured near resting potential is 4.8×10^{-22} (amp)^2. In the spectrum shown in Fig. 3.3.3.-2 of Derksen's study (Derksen, 1965), the fluctuations scaled according to equation 10 yield a value of N of 5.8×10^{-22} (amp)^2 for a Ranvier node (using $r_{mR} = 7 \times 10^7\ \Omega$, as given in the insert of Fig. 3.3.3.-2, and r_{mL} $5 \times 10^5\ \Omega$).

Derksen has reported that changing from normal Ringer to isotonic KCl reduced the intensity of the fluctuations of resting membrane potential of a Ranvier node (Derksen, 1965, Fig. 3.3.3.-2). In the present experiments, the intensity of current fluctuations recorded at $V_m \approx E_K$ was found to increase with increasing $[K]_o$ (Fig. 17). These observations are not necessarily in contradiction. It is well known that an increase in $[K]_o$ generally decreases the resting membrane resistance r_m. If equation 9 holds, it is quite possible that an increase in $\overline{\Delta I_m^2}$ produced by an increase in $[K]_o$ may be accompanied by a decrease in $\overline{\Delta V_m^2}$. Our own data suggest that this might indeed be the case for the lobster axon: increasing $[K]_o$ from 10 to 478 mM increases $\overline{\Delta I_m^2}$ approximately 10-fold for $V_m \approx E_K$ (Fig. 17) while the factor r_m^2 may decrease 100-fold or more. In these conditions, equation 9 would predict a net decrease of $\overline{\Delta V_m^2}$ of approximately 10-fold. It is noteworthy that the data presented by Derksen (Fig. 3.3.3.-2) show that the $1/f$ character of the fluctuations are preserved in isotonic KCl, in agreement with our own measurements.

The present investigation strongly suggests that the coupling between ΔI_m and $\bar{I}_K$

[5] It is recognized that such a comparison may be hazardous. As in the procedure used for normalizing the data recorded from nodes of different areas, one of its implicit assumptions is that the spatial extent of the correlation between the individual sources of fluctuations (e.g. at the molecular level) is much smaller than the dimensions of the node.

is direct, and that the dependence of ΔI_m on g_K and on V_m are indirect, i.e. exist only insofar as changes in g_K and/or V_m affect $\bar{I}_K$. The measurements performed in $[K]_o = 478$ mM, where the nodal membrane possesses a conductance with a region of negative slope, are particularly relevant in this respect. Furthermore, the qualitative agreements between the data obtained on both the Ranvier node and the lobster axon also suggest that these fluctuations are characteristic of the axonal membrane.

The present data have some relevance for the fluctuations of excitability. They do not support the assumption, used in most modelling studies of nerve membrane, of fluctuations which are independent of the mean membrane potential and current and with spectra of the form $1/(f^2 - f^2\alpha)$ (for a review of these studies, see Moore, Perkel, and Segundo, 1966). Furthermore, it is conceivable that the sodium and leakage systems also generate fluctuations which, from the point of view of excitability of the membrane, may also be important. Statistical measurements are more difficult on the sodium system, however, because of its inactivation and the resulting nonstationarity of the underlying process. In this regard, the use of certain agents which have been shown to reduce inactivation, such as DDT, might prove useful (Narahashi and Haas, 1967).

It has been suggested that detailed study of membrane fluctuations might contribute to a better understanding of the intimate nature of membrane processes (Cole, 1968). Some attempts have already been made to consider stochastic versions of the Hodgkin-Huxley equations (FitzHugh, 1955; Lecar and Nossal, 1968). So far, these studies have necessarily been of a theoretical nature since no direct measurements of the fluctuations which could be related to the variables of the Hodgkin-Huxley equations were available.

Random fluctuations with similar spectral characteristics have been observed in a wide variety of electrical devices (for review, see Van Der Ziel, 1959; for a discussion of the mathematical aspects of $f^{-\alpha}$ fluctuations, see Mandelbrot, 1967). It is noteworthy that the intensity of the fluctuations is also frequently related to the mean, DC, current through a power law, with values of m ranging from 0.5 to 4, and more frequently between 1 and 2, not unlike in the present experiments.

The fundamental requirement of any mechanism of $1/f$ fluctuations is the generation of long correlation times. Derksen, in reviewing present theories and known mechanisms of the generation of $1/f$ fluctuations (Derksen, 1965), found none which seemed readily applicable to nerve membrane. However, the model of single file diffusion (Hodgkin and Keynes, 1955) might be worthy of further investigations since it has been shown to exhibit long time constants (Macey and Oliver, 1967).

Additional experimental work and modelling studies are needed in order to fully assess the significance of the fluctuations.

The assistance provided by the members of the Communications Biophysics Group of the Research Laboratory of Electronics, in particular the encouragement and critical comments of Professor Thomas Weiss, is gratefully acknowledged.

This work was supported principally by NIGMS Grant 5 PO1 14940-03.

Support was also received from a graduate fellowship from the Province of Quebec and is gratefully acknowledged.

Received for publication 17 April 1970 and in revised form 28 August 1970.

APPENDIX

Low Noise Voltage Clamping

Practical implementations of the voltage-clamp method usually emphasize high speed of response. However, because of the characteristics of the transresistance amplifier (current-to-voltage transducer) which this method utilizes, a high speed of response is somewhat incompatible with the low noise performance required for measuring the current noise of the membrane.

A simplified incremental model of the experimental configuration used to voltage-clamp a patch of membrane is shown in Fig. 18. The "nodal" membrane is represented as a parallel combination of a capacitance c_m, a resistance r_m, and a current noise source ΔI_m, whose statistics we wish to study as a function of a number of experimental variables. An operational amplifier with infinite input impedance and equivalent input voltage and current noises e_n and i_n (assumed to be uncorrelated) is coupled to the "node" through a feedback resistance r_f (with series Johnson noise source). The resistance of the two axoplasmic "electrodes" in contact with the node are not included. The current electrode can be viewed, however, as lumped with r_f, while the voltage electrode simply contributes an additional Johnson voltage noise which may be lumped with e_n.

In order to achieve the fast rise times required for conventional step-clamp experiments, the nodal membrane must be driven by a source of low impedance. This impedance (the input impedance of the transresistance amplifier) is proportional to r_f and optimum performance is obtained when r_f is a minimum. Its value is limited by the series resistance of the current electrode. Fast rise time and wide bandwidth are obtained, however, at the expense of noise performance. It can be shown that the signal-to-noise ratio of the output of the amplifier is given by

$$\mathrm{S/N} = \frac{\overline{\Delta I_m^2}}{\frac{\overline{e_n^2}}{r_f^2} + \frac{1}{r_f}\left(4KT + \frac{\overline{2e_n^2}}{r_m}\right) + \overline{i_n^2} + \left(\frac{1 + 4\pi^2 f^2 r_m^2 c_m^2}{r_m^2}\right)\overline{e_n^2}}, \qquad (A\,1)$$

where f is the frequency in Hz, K is Boltzmann's constant, and T is the absolute temperature.

Note that S/N improves monotonically with increasing values of r_f. Thus for instance, if the fluctuations of membrane current were a pure Johnson noise, that is, if

$$\overline{\Delta I_m^2} = 4KT/r_m, \qquad (A\,2)$$

an ideal, noiseless ($\overline{e_n^2} = \overline{i_n^2} = 0$) amplifier would yield

$$\mathrm{S/N} = r_f/r_m. \qquad (A\,3)$$

It is apparent, therefore, that optimum rise time and optimum noise performances lead to conflicting requirements of the value of r_f. In a conventional voltage-clamp system, where r_f represents the axoplasmic resistance, equation A 3 predicts a typical S/N of 1/5. With

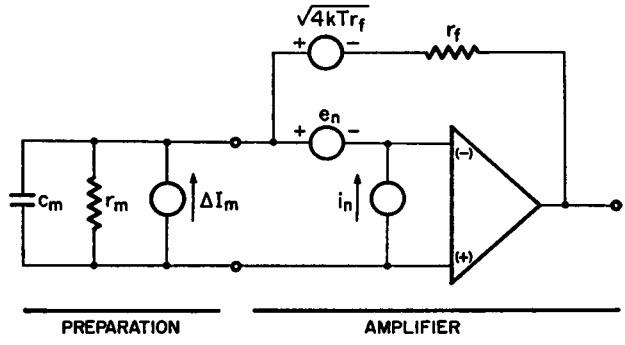

FIGURE 18 Simplified incremental representation of preparation and transresistance amplifier used for recording the steady-state fluctuations of membrane current, ΔI_m, under voltage-clamp conditions.

such a system (even if it were noiseless) the possibility of measuring the fluctuations of membrane current is low.

As the feedback resistance r_f is increased, the contribution of its Johnson noise becomes negligible and equation A 1 tends to

$$S/N = \frac{\overline{\Delta I_m^2}}{\overline{i_n^2} + \dfrac{1 + 4\pi^2 f^2 r_m^2 c_m^2}{r_m^2}\,\overline{e_n^2}}. \qquad (A\,4)$$

It is important to note that the presence of a membrane capacity c_m brings about an effective increase in the undesirable contribution of the voltage noise, $\overline{e_n^2}$, of the amplifier and of the voltage electrode. This increase occurs at the rate of 20 db per decade of frequency above the natural frequency of the nodal membrane, which is of the order of 200 Hz in the lobster axon (see Fig. 3). It is to be expected, therefore, that measurements of membrane fluctuations may become increasingly difficult in the upper audiofrequency range.

Furthermore, as r_f is increased and made large relative to r_m, the need for a second transresistance amplifier to supply the virtual ground to the node (and measure membrane current) disappears. Membrane current can be read off directly from the voltage output of the clamping amplifier, through the factor $-1/r_f$.

REFERENCES

BLAUSTEIN, M. P., and D. E. GOLDMAN. 1966. *J. Gen. Physiol.* **49**:1043.
BRINLEY, F. J. 1965. *J. Neurophysiol.* **28**:742.
CALVIN, W. H., and C. F. STEVENS. 1968. *J. Neurophysiol.* **31**:574.
CHANDLER, W. K., and H. MEVES. 1965. *J. Cell. Comp. Physiol.* **66**:65.
COLE, K. S. 1968. *J. Gen. Physiol.* **51**:1.
DEBECKER, J. C. 1964. *Separatum Experientia.* **20**:553.
DEMKO, P. 1968. Hybrid simulation of the Hodgkin-Huxley model for nerve membrane. S.M. Thesis. Massachusetts Institute of Technology, Cambridge.
DERKSEN, H. E. 1965. *Acta Physiol. Pharmacol. Neer.* **13**:373.
DERKSEN, H. E., and A. A. VERVEEN. 1966. *Science (Washington).* **151**:1388.
DODGE, F. A., B. W. KNIGHT, and J. TOYODA. 1968. *Science (Washington).* **160**:88.
EHRENSTEIN, G., AND D. GILBERT. 1966. *Biophys. J.* **6**:553.
FISHMAN, H. M., and R. I. MACEY. 1969. *Biophys. J.* **9**:140.

FITZHUGH, R. 1955. *Bull. Math. Biophys.* **17**:257.
FRANKENHAEUSER, B. 1957. *J. Physiol. (London).* **137**:245.
FRANKENHAEUSER, B., and A. L. HODGKIN. 1957. *J. Physiol. (London).* **137**:218.
HODGKIN, A. L., and R. D. KEYNES. 1955. *J. Physiol. (London).* **128**:61.
JULIAN, F. J., J. W. MOORE, and D. E. GOLDMAN. 1962 *a. J. Gen. Physiol.* **45**:1195.
JULIAN, F. J., J. W. MOORE, and D. E. GOLDMAN. 1962 *b. J. Gen. Physiol.* **45**:1217.
JUNGE, D., and G. P. MOORE. 1966. *Biophys. J.* **6**:411.
LECAR, H., G. EHRENSTEIN, L. BINSTOCK, and R. E. TAYLOR. 1967. *J. Gen. Physiol.* **50**:1499.
LECAR, H., and R. NOSSAL. 1968. *Biophys. Soc. Annu. Meet. Abstr.* **8**:A132.
MACEY, R. I., and R. M. OLIVER. 1967. *Biophys. J.* **7**:545.
MANDELBROT, B. 1967. *I.E.E.E. (Inst. Elec. Electron. Eng.) Trans. Inform. Theory.* **IT-13**:289.
MOORE, G. P., D. H. PERKEL, and J. P. SEGUNDO. 1966. *Annu. Rev. Physiol.* **28**:493.
MOORE, J. W. 1959. *Nature (London).* **183**:265.
MOORE, J. W., N. ANDERSON, M. BLAUSTEIN, M. TAKATA, J. Y. LETTVIN, W. F. PICKARD, T. BERNSTEIN, and J. POOLER. 1966. *Ann. N.Y. Acad. Sci.* **137**:818.
MUELLER, P. 1958. *J. Gen. Physiol.* **42**:137.
NARAHASHI, T., and H. G. HAAS. 1967. *Science (Washington).* **157**:1438.
NARAHASHI, T., J. W. MOORE, and W. R. SCOTT. 1964. *J. Gen. Physiol.* **47**:965.
PÉCHER, C. 1937. *Compt. Rend. Soc. Biol.* **124**:839.
POUSSART, D. 1966. Quarterly Progress Report No. 81. Research Laboratory of Electronics, Massachusetts Institute of Technology, Cambridge. 213.
POUSSART, D. 1969. *Proc. Nat. Acad. Sci. U.S.A.* **64**:95.
ROJAS, E. R., and I. ATWATER. 1967. *Proc. Nat. Acad. Sci. U.S.A.* **57**:1350.
SPEKREIJSE, H., and H. OOSTING. 1970. *Kybernetik.* **7**:22.
STEIN, R. B. 1967. *Biophys. J.* **7**:797.
TAKATA, M., J. W. MOORE, C. Y. KAO, and F. A. FUHRMAN. 1966. *J. Gen. Physiol.* **49**:977.
TAKATA, M., W. F. PICKARD, J. Y. LETTVIN, and J. W. MOORE. 1966. *J. Gen. Physiol.* **50**:461.
VAN DER ZIEL, A. 1959. Fluctuations Phenomena in Semi-conductors. Academic Press, Inc., New York.
VERVEEN, A. A. 1961. Fluctuation in Excitability. Drukkerij Holland N.V., Amsterdam.
VERVEEN, A. A. 1962. *Acta Physiol. Pharmacol. Neer.* **11**:268.
VERVEEN, A. A., and H. E. DERKSEN. 1965. *Kybernetik.* **2**:152.
VERVEEN, A. A., and H. E. DERKSEN. 1968. *Proc. I.E.E.E. (Inst. Elec. Electron. Eng.)* **56**:906.
VERVEEN, A. A., and H. E. DERKSEN. 1969. *Acta Physiol. Pharmacol. Neer.* **15**:353.
VERVEEN, A. A., H. E. DERKSEN, and K. L. SCHICK. 1967. *Nature (London).* **216**:586.